

# Models and Methods for Free Material Optimization with Local Stress Constraints

Alemseged Gebrehiwot Weldeyesus\*

## Abstract

Free Material Optimization (FMO) is a powerful approach of structural optimization of composite structures leading to conceptual optimal designs. The design variable is the elastic material tensor which is allowed to change its values freely over the design domain giving optimal material properties and optimal material distribution. The only requirements are that the stiffness tensor is forced to be symmetric positive semidefinite as a necessary condition for its physical attainability. One of the goals of this article is to introduce constraints on local stresses to existing FMO problems for laminated plates and shells and propose new stress constrained FMO problem formulations. The FMO problems are non convex semidefinite program with a special structure involving many small matrix inequalities. This structure is exploited by our special purpose optimization method. The second goal of this article is to extend primal-dual interior point method for classical FMO problems to stress constrained FMO problems. The numerical experiments show that the optimal solutions to the stress constrained problems can be achieved within a moderate number of iterations. The local stress constraints are satisfied with high accuracy. The method and models are supported by numerical examples.

**Mathematics Subject Classification 2010:** 90C22, 90C90, 74P05, 74P15

**Keywords:** Structural optimization, free material optimization, nonlinear semidefinite optimization, stress constraints

---

The research was partially funded by the Danish Council for Strategic Research through the *Danish Center for Composite Structures and Materials* (DCCSM).

\*DTU Wind Energy, Technical University of Denmark, Frederiksborgvej 399, 4000 Roskilde, Denmark. E-mail: alwel@dtu.dk

# 1 Introduction

Free Material Optimization (FMO) deals with obtaining a composite structure with optimal material properties and optimal material distribution that can sustain a given set of loads. Such optimal structures can be considered as ultimately best structures among all possible elastic continua [36]. These optimal designs can also be used as benchmarks with which other designs obtained by other approaches of structural optimization can be compared.

The basic concept of FMO can be traced back to the early 1990s in [2], [3], and [22]. Since then there are several research studies dealing with more advanced FMO models. FMO formulations have been extended to include a wide range of constraints such as constraints on local stresses, local strains, displacement and fundamental frequencies in e.g. [17], [15], [11], and [25]. Theoretical aspects of FMO problems including existence of optimal solutions are analyzed in different studies [11] and [34]. There are also numerical optimization methods proposed in several articles [36], [14], [24], [27], [26], and [33].

High stresses are one of the causes for engineering structures to fail. The scope of several studies in structural optimization are extended to control stresses within a certain limit in the optimal structures. However, addressing stresses in the optimization problem is not straight forward. The choice of optimization problem formulation with relevant stress criteria and the development of methods that can computationally handle the problems are some of the main challenges.

Topology optimization is one of the research fields that has been extensively studied. For stress-based topology optimization see [35], [23], [5], [7], [20], and [18] for continua, and [13], [10], [29], and [30] for trusses and the references therein. Stresses are addressed in topology optimization in several ways. One way is limiting the stresses by introducing stress constraints which can be local at element level or global by aggregating the stresses in the design. Adding such constraints however leads to optimization problems that are difficult to solve. Suitable mathematical properties such as convexity are lost. Moreover, the problems face the singularity phenomenon described in e.g. [13] and [1] among many others.

FMO problems with stress constraints are analyzed and solved in [17], [16], and [15] for two-dimensional and in [11] for three-dimensional structures. The constraints are introduced with a term of an integral of the norm of the stresses. One of the outcome of FMO models is that higher stresses are primarily removed by changing material properties. This is unlike to other approaches in structural optimization where the materials are fixed and higher stresses are avoided by other ways, for e.g., changing the geometry of the optimal structure. The result is supported by making a comparison between solutions to FMO problem and the classical Variable Thickness Sheet (VTS) problem in [15].

The stress constraints in FMO defined in e.g. [15] are highly nonlinear involving the design variable stiffness tensor. This makes the level of the difficulty to solve stress constrained FMO problems even worse. The stress constrained FMO problems in [15], [17], and [16] are solved with the method based on Augmented Lagrangian function in [14] and [24]. The problems in [11] are solved by one of the recent methods based on sequential convex programming developed in [27, 26]. The method in general requires large number of iterations. The original setting of the problems were approximated by problems where the stress constraints are removed and added to the objective function using a penalty term. The solutions to the new approximation problems are of high quality. However, the feasibility tolerance of the stress constraint is moderate.

The focus of this article is on FMO formulations with constraints on local stresses. As far as to our knowledge there are no analogous FMO formulations with stress constraints for laminated structures. In [32], FMO problems for laminated plates and shells are proposed based on the formulations in [9]. One of the objective of this article is to introduce constraints on local stresses to these formulations and propose FMO problem formulations with local stress constraints for laminates.

The necessary condition for physical attainability of the stiffness tensor results in matrix inequalities in the optimization problem. Therefore, FMO problems belong to a class of SemiDefinite Program (SDP). Recently, an efficient primal-dual interior point method with special purpose to FMO problems is developed in [33]. The method is generalized for FMO models for laminated plates and shells in [32]. It exploits the special structure that FMO problems have many but small matrix inequality constraints. Solutions are reported to the largest classical FMO problems solved to date. It requires a modest number of iterations that almost does not increase with problem size. The second objective of this article is to show that a slightly modified version of this method can successfully solve the stress constrained problems of this article. The stress constraints are treated in the algorithm keeping their original settings in the problem formulations. The numerical experiments show that the solutions are obtained in moderate number of iterations with higher accuracy.

The organization of the article is as follows. In Section 2 we formulate the finite dimensional FMO problems with stress constraints for both solid and laminated structures. In Section 3 we present the implementation of the algorithm and the slight modification introduced to the method described in detail in [33]. We report and explain the results of the performed numerical experiments in Section 4. The conclusions and possibly future research works are presented in Section 5.

## 2 Problem formulations

In this section we present FMO problem formulations with stress constraints for solid and laminated plate and shell structures. In both cases we start with the discrete version of the classical minimum compliance (maximum stiffness) and the minimum weight FMO formulations. For details on the problem formulations and finite element discretization, see [27] and [17] for solid structures, and [32], [9], and [4] for laminated structures.

It is pointed out in e.g. [15] that addressing stress constraints in structural optimization using FMO is a challenge. In the first place, there is no existing general failure criterion. The realization of the optimal structure is also important in using one of the several existing failure criteria, for example see [12] for different failure criteria in fiber reinforced composites. Moreover, in FMO material properties are also design variables giving conceptual optimal designs. Despite these challenges we follow the measure proposed in [15] which is the norm of the stresses integrated over the finite element in the discrete problems.

In FMO problem formulations the requirement of the physical attainability of the stiffness tensor is introduced by matrix inequality constraints. As a measure of stiffness the trace of the elastic stiffness tensor is used. It is locally bounded from above by  $\bar{\rho}$  to avoid arbitrarily stiff materials and from below by  $\underline{\rho}$  to limit the extent of softness. These bounds must satisfy the relation  $0 \leq \underline{\rho} < \bar{\rho} < \infty$ . We consider  $n_L$  given external static nodal load vectors  $f_\ell \in \mathbb{R}^n$ , where  $\ell \in L = \{1, \dots, n_L\}$  and  $n$  is the number of finite element degrees of freedom. We prescribe weights  $w_\ell$  for the loads  $f_\ell$  satisfying  $\sum_\ell w_\ell = 1$  and  $w_\ell > 0$  for each  $\ell \in L$ .

Next, we present the FMO problems with local constraints for solids and laminated structures. In both cases we follow similar approach. We first formulate the problems without stress constraints. Then, we define the stress constraints and include in the unconstrained problems to formulate the stress constrained FMO problems.

### 2.1 FMO for solid structures

This section is essentially identical to the corresponding section in [33] and is included for completeness. We consider a design domain  $\Omega$  partitioned in to  $m$  uniform finite elements  $\Omega_i$  for  $i = 1, \dots, m$ . The elastic stiffness tensor  $E(x)$  is approximated by a function that is constant on each finite element with its element values making the vector of block matrices  $E = (E_1, \dots, E_m)^T$ . For any given external static nodal load vectors  $f_\ell$ , the associated displacement  $\mathbf{u}_\ell$  must satisfy the linear elastic equilibrium equation

$$\mathbf{A}(E)\mathbf{u}_\ell = \mathbf{f}_\ell, \ell \in L, \tag{1}$$

where the stiffness matrix  $\mathbf{A}(\mathbf{E})$  is given by

$$\mathbf{A}(\mathbf{E}) = \sum_{i=1}^m \mathbf{A}_i(\mathbf{E}), \quad \mathbf{A}_i(\mathbf{E}) = \sum_{k=1}^{n_G} \mathbf{B}_{i,k}^T \mathbf{E}_i \mathbf{B}_{i,k}. \quad (2)$$

The matrices  $\mathbf{B}_{i,k}$  are (scaled) strain-displacement matrices computed from the derivative of the shape functions and  $n_G$  is the number of Gaussian integration points, see e.g. [6].

We define the set of admissible materials  $\tilde{\mathcal{E}}$  by

$$\tilde{\mathcal{E}} := \{ \mathbf{E} \in (\mathbb{S}_+^d)^m \mid \underline{\rho} \leq \text{Tr}(\mathbf{E}_i) \leq \bar{\rho}, i = 1, \dots, m \} \quad (3)$$

where the space  $\mathbb{S}_+^d$  is the cone of positive semidefinite matrices in the space  $\mathbb{S}^d$  of symmetric  $d \times d$  matrices, i.e.,  $\mathbf{E}_i \in \mathbb{S}_+^d$  if and only if  $\mathbf{E}_i = \mathbf{E}_i^T$  and  $\mathbf{E}_i \succeq 0$ . The exponent  $d$  takes the value 3 for two-dimensional problems and 6 for three-dimensional problems.

Next, we formulate FMO problems for solids without stress constraints. The primal minimum compliance FMO problem is formulated as

$$\begin{aligned} & \underset{\mathbf{u}_\ell \in \mathbb{R}^n, \mathbf{E} \in \tilde{\mathcal{E}}}{\text{minimize}} && \sum_{\ell \in L} w_\ell \mathbf{f}_\ell^T \mathbf{u}_\ell \\ & \text{subject to} && \mathbf{A}(\mathbf{E}) \mathbf{u}_\ell = \mathbf{f}_\ell, \ell \in L, \\ & && \sum_{i=1}^m \text{Tr}(\mathbf{E}_i) \leq V. \end{aligned} \quad (4)$$

The constant  $V > 0$  is an upper bound on the amount of resource material to distribute in the structure and satisfies the relation

$$\sum_{i=1}^m \underline{\rho} < V < \sum_{i=1}^m \bar{\rho}.$$

The primal minimum weight FMO problem is

$$\begin{aligned} & \underset{\mathbf{u}_\ell \in \mathbb{R}^n, \mathbf{E} \in \tilde{\mathcal{E}}}{\text{minimize}} && \sum_{i=1}^m \text{Tr}(\mathbf{E}_i) \\ & \text{subject to} && \mathbf{A}(\mathbf{E}) \mathbf{u}_\ell = \mathbf{f}_\ell, \ell \in L, \\ & && \sum_{\ell=1}^L w_\ell \mathbf{f}_\ell^T \mathbf{u}_\ell \leq \gamma. \end{aligned} \quad (5)$$

The weighted multiple load non convex FMO problems (4) and (5) are of Simultaneous ANalysis and Design (SAND) formulation without stress constraints.

Theories and methods for problems (4) and (5) and/or their minimax formulations have been extensively studied in several articles, see [28], [28], [34] and the references therein. By applying the Schur complement theorem the problems can be written as linear problems, but result in large matrix inequalities that can hardly be handled computationally [17]. Under the mild assumption  $E \succ 0$  on the elastic stiffness tensor the stiffness matrix  $\mathbf{A}(\mathbf{E})$  is nonsingular [28]. Therefore, by solving the displacement in the equilibrium equation (1), it can be eliminated from the problems (4) and (5) and then equivalent nested convex formulations can be derived. The SAND formulations are the preferred choices in this article. This is due to the numerical experiments in [33] and it is more convenient to track numerically the stress constraints in the SAND formulations than in the nested formulations for a second order method.

Now, we introduce the stress constraints. We determine the norm of the stress due to the load  $\mathbf{f}_\ell$  integrated over  $i$ th element by

$$\|\boldsymbol{\sigma}_{i,\ell}\|^2 := \int_{\Omega_i} \|\boldsymbol{\sigma}_\ell\|^2 d\Omega = \sum_{k=1}^{n_G} \|\mathbf{E}_i \mathbf{B}_{ik} \mathbf{u}_\ell\|^2. \quad (6)$$

We then include in problems (4) and (5) the constraints on local stresses

$$\|\boldsymbol{\sigma}_{i,\ell}\|^2 \leq s_\ell, \quad \text{for each } \ell \in L \text{ and } i = 1, \dots, m. \quad (7)$$

The upper bound  $s_\ell$  is estimated first by solving the corresponding unconstrained problems (4) and (5) and scaling the maximum stress norm by a factor  $k \in (0, 1)$ , i.e.,

$$s_\ell = k \max_i \{\|\boldsymbol{\sigma}_{i,\ell}\|^2\}. \quad (8)$$

The existence of optimal solution to the stress constrained FMO problems is shown in [11] under natural assumptions.

## 2.2 FMO for laminated plates and shells

This section is mostly adopted from Subsection 2.3 of [32] and is included for the completeness and ease of readability. In laminated structures mechanical properties are usually determined with respect to a reference midsurface, denoted by  $\omega$ . In order to formulate the finite dimensional problem,  $\omega$  is partitioned in to  $m$  uniform finite elements  $\omega_i$  for  $i = 1, \dots, m$ . As in the case of solid structures the plane-stress in-plane elastic stiffness tensor  $\mathbf{C}$  and transverse tensor  $\mathbf{D}$  are approximated by functions constant on each element in each layer. The  $i$ th element values of the stiffness tensors  $\mathbf{C}$  and  $\mathbf{D}$  on the  $l$ th layer are denoted by  $\mathbf{C}_{il}$  and  $\mathbf{D}_{il}$  respectively.

Given external static nodal load vectors  $f_\ell$  the resulting displacement  $(\mathbf{u}, \boldsymbol{\theta})_\ell$  (translational and rotational) satisfies the elastic equilibrium equation

$$\mathbf{K}(\mathbf{C}, \mathbf{D})(\mathbf{u}, \boldsymbol{\theta})_\ell = \mathbf{f}_\ell, \ell \in L, \quad (9)$$

where  $\mathbf{K}(\mathbf{C}, \mathbf{D})$  the stiffness matrix is given by

$$\mathbf{K}(\mathbf{C}, \mathbf{D}) = \sum_{i=1}^m (\mathbf{K}_i^\gamma(\mathbf{C}) + \mathbf{K}_i^{\gamma\chi}(\mathbf{C}) + (\mathbf{K}_i^{\gamma\chi}(\mathbf{C}))^T + \mathbf{K}_i^\chi(\mathbf{C}) + \mathbf{K}_i^\zeta(\mathbf{D})). \quad (10)$$

The element stiffness matrices in (10) are given by

$$\mathbf{K}_i^\gamma(\mathbf{C}) = \sum_{l,(j,k) \in n_i} \int_{\omega_i} t_{il} (\mathbf{B}_{jl}^\gamma)^T \mathbf{C}_{il} \mathbf{B}_{kl}^\gamma dS \quad (11a)$$

$$\mathbf{K}_i^{\gamma\chi}(\mathbf{C}) = \sum_{l,(j,k) \in n_i} \int_{\omega_i} \tilde{t}_{il} (\mathbf{B}_{jl}^\gamma)^T \mathbf{C}_{il} \mathbf{B}_{kl}^\chi dS \quad (11b)$$

$$\mathbf{K}_i^\chi(\mathbf{C}) = \sum_{l,(j,k) \in n_i}^N \int_{\omega_i} \tilde{\tilde{t}}_{il} (\mathbf{B}_{jl}^\chi)^T \mathbf{C}_{il} \mathbf{B}_{kl}^\chi dS \quad (11c)$$

$$\mathbf{K}_i^\zeta(\mathbf{D}) = \kappa \sum_{l,(j,k) \in n_i} \int_{\omega_i} t_{il} (\mathbf{B}_{jl}^\zeta)^T \mathbf{D}_{il} \mathbf{B}_{kl}^\zeta dS, \quad (11d)$$

where  $n_i$  is the index set of nodes associated with the element  $\omega_i$ . The matrices  $\mathbf{B}_{il}^\gamma$ ,  $\mathbf{B}_{il}^\chi$  and  $\mathbf{B}_{il}^\zeta$  are the (scaled) strain-displacement matrices for membrane strains, for bending strains, and for shear strains, respectively. The factors  $t_{il}$ ,  $\tilde{t}_{il}$  and  $\tilde{\tilde{t}}_{il}$  are computed as

$$\begin{aligned} t_{il} &= t_{il}^b - t_{il}^a, \quad \tilde{t}_{il} = \frac{1}{2}((t_{il}^b)^2 - (t_{il}^a)^2), \\ \tilde{\tilde{t}}_{il} &= \frac{1}{3}((t_{il}^b)^3 - (t_{il}^a)^3), \end{aligned} \quad (12)$$

where  $t_{il}^b$  and  $t_{il}^a$  the upper and lower transverse coordinates of the  $l$ th layer at the center of the element  $\omega_i$ . The coefficient  $\kappa < 1$  appearing in the shear term in (11d) is the shear correction factor. This is to take into account the shell model which is used in applications.

Given that the laminate has  $N$  number of layers we define the set of admissible

material  $\tilde{\mathcal{E}}$  by

$$\tilde{\mathcal{E}} = \left\{ (\mathbf{C}, \mathbf{D}) \in (\mathbb{S}_+^3)^{mN} \times (\mathbb{S}_+^2)^{mN} \mid \right. \\ \left. \rho \leq t_{il} (\text{Tr}(\mathbf{C}_{il}) + \frac{1}{2}\text{Tr}(\mathbf{D}_{il})) \leq \bar{\rho}, \quad i = 1, \dots, m, l = 1, \dots, N \right\}. \quad (13)$$

Now, we formulate the unconstrained problems. The primal minimum compliance FMO formulation is then stated as

$$\begin{aligned} & \underset{(\mathbf{u}, \boldsymbol{\theta})_\ell \in \mathbb{R}^n, (\mathbf{C}, \mathbf{D}) \in \tilde{\mathcal{E}}}{\text{minimize}} && \sum_{\ell \in L} w_\ell (\mathbf{f}_\ell)^T (\mathbf{u}, \boldsymbol{\theta})_\ell \\ & \text{subject to} && \mathbf{K}(\mathbf{C}, \mathbf{D})(\mathbf{u}, \boldsymbol{\theta})_\ell = \mathbf{f}_\ell, \quad \ell \in L, \\ & && \sum_{i=1}^m \sum_{l=1}^N t_{il} \left( \text{Tr}(\mathbf{C}_{il}) + \frac{1}{2}\text{Tr}(\mathbf{D}_{il}) \right) \leq V, \end{aligned} \quad (14)$$

with the volume bound  $V > 0$  satisfying

$$\sum_{l=1}^N \sum_{i=1}^m \rho < V < \sum_{l=1}^N \sum_{i=1}^m \bar{\rho}.$$

The discrete primal minimum weight FMO formulation is

$$\begin{aligned} & \underset{(\mathbf{u}, \boldsymbol{\theta})_\ell \in \mathbb{R}^n, (\mathbf{C}, \mathbf{D}) \in \tilde{\mathcal{E}}}{\text{minimize}} && \sum_{i=1}^m \sum_{l=1}^N t_{il} \left( \text{Tr}(\mathbf{C}_{il}) + \frac{1}{2}\text{Tr}(\mathbf{D}_{il}) \right) \\ & \text{subject to} && \mathbf{K}(\mathbf{C}, \mathbf{D})(\mathbf{u}, \boldsymbol{\theta})_\ell = \mathbf{f}_\ell, \quad \ell \in L, \\ & && \sum_{\ell \in L} w_\ell (\mathbf{f}_\ell)^T (\mathbf{u}, \boldsymbol{\theta})_\ell \leq \gamma. \end{aligned} \quad (15)$$

Next, we present our motivation for the type of stress constraints that we introduce to the problems (14) and (15).

It is known from mechanics of laminated structures that stresses vary across the thickness of the laminate with linear variation within a layer (we are talking about linear elasticity). Therefore, we make two stress evaluations in each layer over each element  $\omega_i$ , at the top and lower transverse coordinates of the layer. This allows us to capture the stress extremities within each layer and each element. We follow similar approach proposed for solids and make these evaluations by the integral form of stresses, i.e., analogous to (6). The stress due to the load

$\mathbf{f}_\ell$  on the  $i$ th element at the bottom of the  $l$ th layer is

$$\begin{aligned} \|\boldsymbol{\sigma}_{il,\ell}^a\|^2 &:= \int_{\omega_i} \|\boldsymbol{\sigma}_{i,\ell}^a\|^2 d\omega = \\ &\sum_{k=1}^{n_G} \left( \|\mathbf{C}_{il}(\mathbf{B}_{ikl}^\gamma(\mathbf{u}, \boldsymbol{\theta})_\ell + t_{il}^a \mathbf{B}_{ikl}^X(\mathbf{u}, \boldsymbol{\theta})_\ell)\|^2 + \|\mathbf{D}_{il} \mathbf{B}_{ikl}^\zeta(\mathbf{u}, \boldsymbol{\theta})_\ell\|^2 \right). \end{aligned}$$

and the top of the  $l$ th layer is

$$\begin{aligned} \|\boldsymbol{\sigma}_{il,\ell}^b\|^2 &:= \int_{\omega_i} \|\boldsymbol{\sigma}_{i,\ell}^b\|^2 d\omega = \\ &\sum_{k=1}^{n_G} \left( \|\mathbf{C}_{il}(\mathbf{B}_{ikl}^\gamma(\mathbf{u}, \boldsymbol{\theta})_\ell + t_{il}^b \mathbf{B}_{ikl}^X(\mathbf{u}, \boldsymbol{\theta})_\ell)\|^2 + \|\mathbf{D}_{il} \mathbf{B}_{ikl}^\zeta(\mathbf{u}, \boldsymbol{\theta})_\ell\|^2 \right). \end{aligned}$$

Then, we propose the following stress constraints for laminated plates and shells

$$\begin{aligned} \|\boldsymbol{\sigma}_{il,\ell}^a\|^2 &\leq s_\ell, \quad \ell \in L, \quad i = 1, \dots, m, \text{ and } l = 1, \dots, N, \\ \|\boldsymbol{\sigma}_{il,\ell}^b\|^2 &\leq s_\ell, \quad \ell \in L, \quad i = 1, \dots, m, \text{ and } l = 1, \dots, N, \end{aligned} \tag{16}$$

with the value of  $s_\ell$  is determined as in (8).

In [9], FMO problem formulations with similar structures to the problems (14) and (15) but for a *single* layer are studied and existence of optimal solution is proved. However, there is no sufficient theoretical background in the literature to guarantee the result for multilayer laminates. The case is even worse when the stress constraints in (16) are included to these problems. The theoretical aspect of these problems need to be further investigated. Any outcome of this article regarding the stress constrained FMO problems for laminates is only the result of numerical experiments.

### 3 Optimization method and implementation

The FMO problems (4), (5), (14), and (15) all have linear objective functions with matrix inequalities and nonlinear (and non convex) vector constraints. Therefore, they are classified as non convex SDPs. In general, FMO problems tend to be large-scale problems for a reasonable mesh size. This is because the design variable is the stiffness tensor at each point of the design domain. However, the special property that the matrix inequalities are small (but many) can be exploited with a special purpose optimization method. An efficient primal-dual method with special purpose to FMO is developed in [33]. The method has shown success in solving by far the largest FMO problems of formulations in (4) and (5)

and some other equivalent formulations. It is also generalized in [32] to solve the FMO problems for laminates of the formulation in (14).

Stress constrained structural optimization problems are in general difficult problems to solve and usually computationally expensive. The problems may not also satisfy constraint qualifications [1], stated as singularity phenomenon in [13]. The stress constraints for FMO problems in (7) and (16) are highly nonlinear in the stiffness tensor and displacement. Hence, the challenge in the handling of computations and finding accurate solutions rises to a complex issue in FMO problems with stress constraints.

In this article we slightly modify the primal-dual interior point method developed in [33] and [32] to solve the stress constrained problems. We employ a perturbation to the the coefficient matrix of the saddle point system that results during applying Newton's method to solve the optimality conditions. This is based on inertia controlling methods [19, 8, 31] to ensures that a search direction gives a decrease in the merit function chosen in the algorithm.

The stress constraints are treated in the algorithm directly keeping their original settings in (7) and (16). In other studies these are often moved to the objective function using a penalty term [27, 26]. The code is entirely implemented in MATLAB. The standard QUAD4 bilinear elements obtained by full Gaussian integration are considered for the two-dimensional problems. For the laminate problems we consider the standard quadrangular CQUAD4 elements with six degrees of freedom per node with full Gaussian integration layer wise and explicit integration over the thickness. The overview of algorithmic parameters are described in [33] and [32].

## 4 Numerical experiments

For the numerical experiments we consider the minimum compliance problems (4) together with stress constraints (7) for two-dimensional problems, and (14) together with the stress constraints (16) for problems on laminated structures. The total weight fraction is set to 40% of the maximum possible weight and the bounds on the traces of the stiffness tensors are scaled such that  $\bar{\rho}/\underline{\rho} = 10^5$ .

Through out this section we use the color scale with limits  $\underline{\rho}$  and  $\bar{\rho}$  given in Figure 1 for all plots of the optimal density distribution. We use own color scales for plots of optimal stress norms to easily show high stresses in the unconstrained problems and regions of active stress constraints in the constrained problems. Note that the labels of the color bar are the norm of the stresses, not the norm of the stresses squared, as used in Table 3. For the two-dimensional Examples 4.1 and 4.2 we also report the principal stress directions which are computed as principal eigenvectors associated to the Voigt-stress tensor.



Figure 1: Color bar for the plots of optimal density distribution.

There are five examples in this section. The first two examples are for two-dimensional problems and the last three examples are for laminated structures. In Example 4.1 we consider L-shaped design domain of dimension (normalized)  $1 \times 1$  and a quarter removed from one of the corners. In Example 4.2 we consider a Michell beam problem on a rectangular design domain of dimension  $2 \times 1$ . For the examples on laminates we consider a laminate spanning a region of dimension  $1 \times 1$  for the clamped plates in Examples 4.3 and 4.4, and  $1 \times 8$  for the shell beam in Example 4.5. The ratio of the thickness to the shortest dimension is 0.01 and is distributed evenly for layered laminates. Layers are numbered in the thickness direction from bottom to top. The problem instances are presented in Tables 1 and 2.

The numerical results are reported in Table 3 listing some comparisons between solving the constrained and unconstrained problems. The optimality tolerances are the norm of the first-order optimality conditions measured without perturbation on the complementarity conditions. By feasibility tolerances we also refer to the feasibility of the stress constraints in the original problem settings (7) and (16). Looking at the numerical values the active stress constraints are feasible with high accuracy. The solutions to the unconstrained problems are obtained within 30 and 61 iterations where as within 85 and 142 for the constrained problems. This can be considered as modest taking in to account that the problems are nonlinear SDPs. Moreover, the number of iterations is modest compared to the results in other literatures, see for example [16] for two dimensional, and [11] for three-dimensional problems. The increase in the number of iterations in solving the constrained problems is expected since the stress constraints are nonlinear involving matrix variables. It is common practice in structural optimization that stresses are reduced at the cost of an increase in compliance. This is also shown in Table 3 for FMO problems. However, the surprising outcome from the numerical experiments is that compliances are worsened not significantly in FMO. In all examples the increase in compliance is less than 5% while stresses are reduced by more than 50%

In all cases, higher stresses near the fixed or loaded regions in the unconstrained problems are avoided in the constrained problems. For a physically meaningful chosen values of the scaling factor  $k$  in (8), the stress constraints are found to be active in wider stiff regions of the optimal designs in the constrained

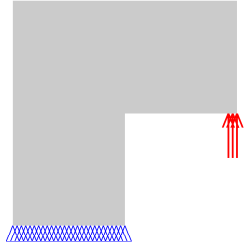


Figure 2: Design domain, boundary condition, and external load for the L-shape design domain.

problems. The similarity between the optimal density distributions for the constrained and unconstrained problems imply that stresses are primarily reduced in FMO by changing material properties. The case is different in other structural optimization approaches where material properties are fixed which and there is less freedom than in FMO. Therefore, the stresses are reduced by other means such as changing the geometry of the topology. Similar results can be found in, e.g., [15], [16], and [17].

**Example 4.1.** We consider the two-dimensional FMO problem on L-shaped design domain from [15], see Figure 2. When solving the problem without stress constraints, we can see the much higher stresses around the reentrant corner, Figure 4a. This is actually typical example giving stress singularity in the reentrant corner. For this case we can allow least value of the scaling factor  $k$  in (8) than in the rest of the examples of this article. It can be seen in Figure 4b the high stresses are avoided. However, looking at the optimal density distributions in Figure 3 the difference is not that big. The higher stress are reduced by reinforcing the reentrant corner with materials forming smooth-like arcs, see the zoom-in Figure 5b of the region. In general, these results closely agree with the results in [15].

**Example 4.2.** In this example we consider the classical two-dimensional Michell beam problem as shown in Figure 6. In the solution to the unconstrained problem there are higher stresses around the two ends of the fixed edge, see Figure 8a. These stresses are reduced in the constrained problem, Figure 8b. Similar to the previous example, there is no much difference in the optimal density distributions between the solutions to the constrained and unconstrained problems, see Figure 7. The reduction of the higher stresses is mainly accomplished by changing the material directions around these regions. The direction changing materials around these regions in Figure 9a in the unconstrained problem are replaced by unidirectional-like materials in Figure 9b in the constrained problem.

Table 1: FMO problem instances for the two-dimensional problems.

Problems	No. of FEs	No. stress constraints	No. of linear matrix inequalities	No. of design variables	No. of non-fixed state variables
L-shape	7500	7500	7500	45000	15300
Michell beam	20000	20000	20000	120000	40400

Table 2: FMO problem instances for the laminate problems.

Problems	No. of layers	No. of FEs	No. stress constraints	No. of linear matrix inequalities	No. of design variables	No. of non-fixed state variables
Clamped plate (pressure load)	8	2500	40000	40000	180000	14406
Clamped plate (central load)	8	2500	40000	40000	180000	14406
Shell beam (two load cases)	1	12800	51200	25600	115200	76320

Table 3: Numerical results for the problem instances in Tables 1 and 2 and the minimum compliance problems (4) and (14) with the stress constraints (7) and (16) respectively. (Compliance and stress norms are scaled)

Problems	Without stress constraints				With stress constraints				
	Iter	Compl- iance	Max. tress norm	Opt/feas tolerances	k	Iter	Compl- iance	Max. stress norm	Opt/feas tolerances
L-shape	30	1.8951	1.3206	2.7e-08/4.0e-10	0.2	85	1.9281	0.2643	9.5e-08/8.9e-09
Michell Beam	47	2.4427	1.9372	8.1e-08/1.7e-11	0.4	102	2.4579	0.7749	8.5e-08/4.3e-10
Clamped plate (pressure load)	47	5.4771	2.1574	3.4e-07/6.9e-09	0.5	115	5.5624	1.0783	6.5e-06/8.8e-07
Clamped plate (central load)	54	7.1531	9.3224	3.5e-07/3.0e-08	0.5	138	7.1876	4.6612	3.7e-07/9.6e-09
Shell beam (two load cases)	61	6.5645	0.1370	7.6e-07/5.9e-09	0.4	142	6.7257	0.0548	3.4e-07/7.9e-10

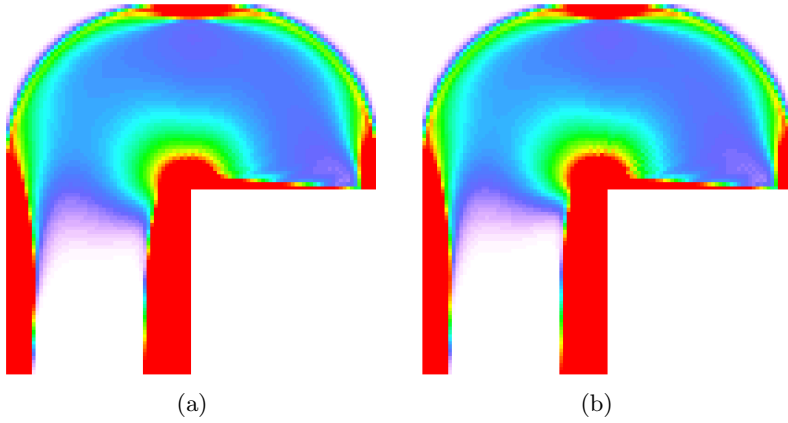


Figure 3: Optimal density distributions of the L-shape problem, (a) without stress constraints, (b) with stress constraints.

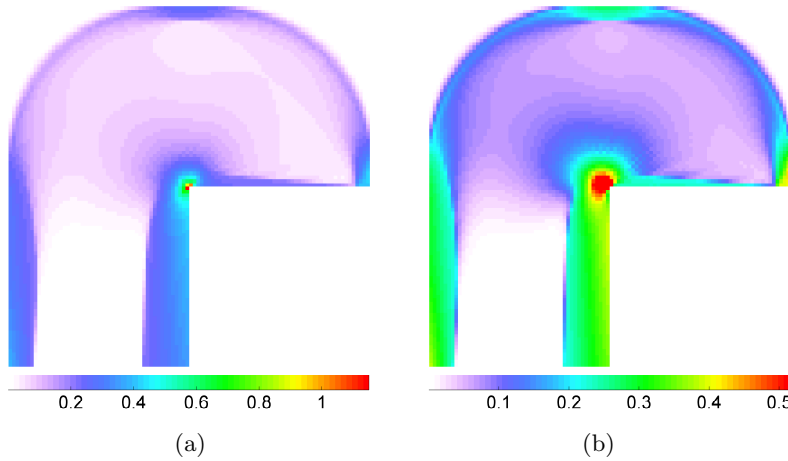


Figure 4: Optimal stress norms for the L-shape problem, (a) without stress constraints, (b) with stress constraints.

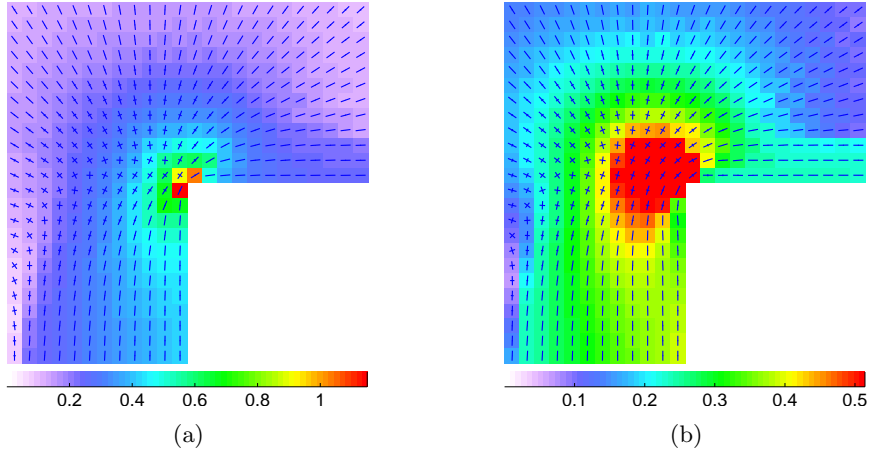


Figure 5: Optimal principal stresses around the reentrant corner for the L-shape problem, (a) without stress constraints, (b) with stress constraints.



Figure 6: Design domain, boundary condition, and external load for the Michell beam problem.

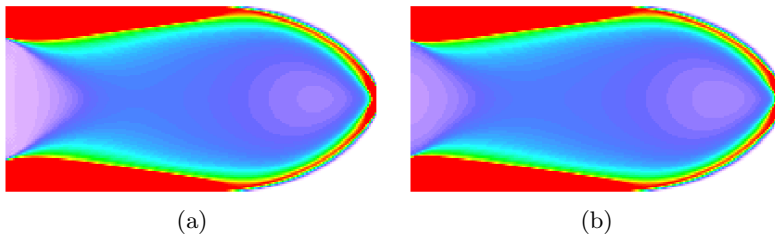


Figure 7: Optimal density distributions for the Michell beam problem, (a) without stress constraints, (b) with stress constraints.

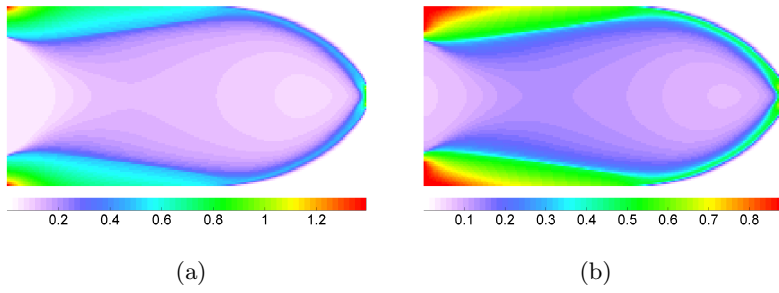


Figure 8: Optimal stress norms for the Michell beam problem, (a) without stress constraints, (b) with stress constraints.

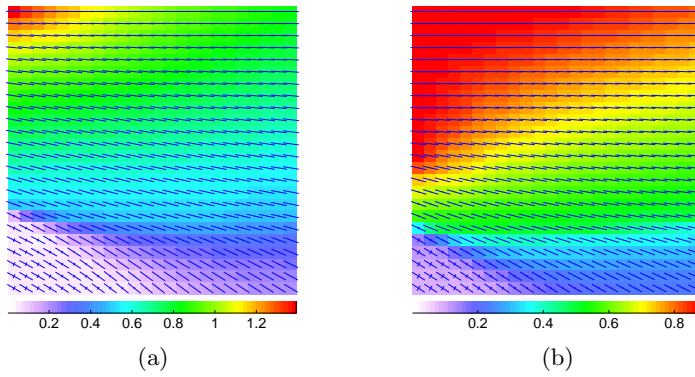


Figure 9: Optimal principal stresses around the upper left corner for the Michell beam problem, (a) without stress constraints, (b) with stress constraints.

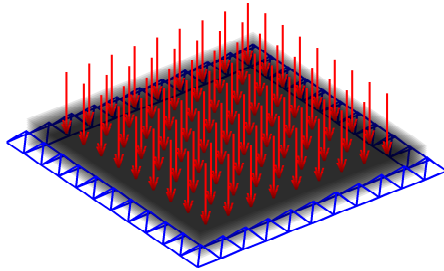


Figure 10: Design domain, boundary condition, and external load for the clamped plate with pressure load.

**Example 4.3.** We consider a clamped plate of eight layers loaded uniformly, see Figure 10. In this case the optimal solution corresponds to a sandwich-like symmetric laminate. Therefore, we report results only for the bottom four layers. Looking at the density distributions in Figure 11, we notice a slight visible difference in the middle four layers where some more materials are used around the fixed regions in the constrained problem than in the unconstrained problem. Figure 12 shows that there are higher stresses in the surface layers mainly concentrated around the fixed four edges of the plate. These are controlled to be within the limit in the constrained problem, Figure 13.

In our model we follow the First Order Deformation Theory (FSDT), see [21], in which the out-of-plane shear stresses are taken in to account. Unlike the two-dimensional problems, reporting the mechanism by which high stress are avoided is not straight forward for laminates. Hence, the realization of the solutions to FMO problems for laminates needs further investigation. This applies to examples 4.3, 4.4 and 4.5 of this article.

**Example 4.4.** We consider a similar case as example 4.3, a clamped laminate of eight plate layers but with the load concentrated at the center, see Figure 14. This is to consider a situation where local higher stresses are located around the loaded area. The solution again gives a sandwich-like symmetric laminate with the stiff area around the center appearing in all layers. The plots are for the first four layers. In the unconstrained problem we can see from Figure 16 that there are higher stresses in a small region around the center and mainly in the surface layers. These are avoided in the constrained problem 17 and all layers around

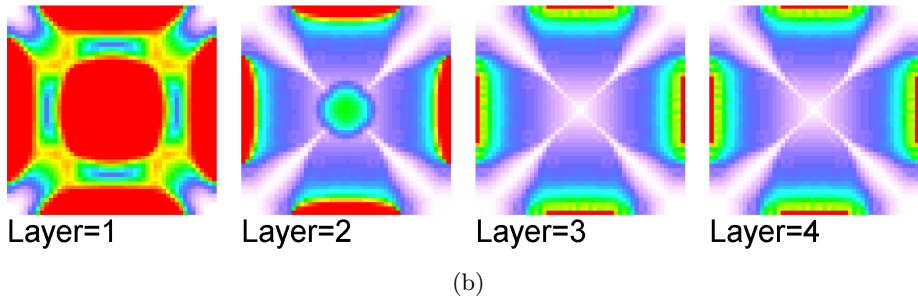
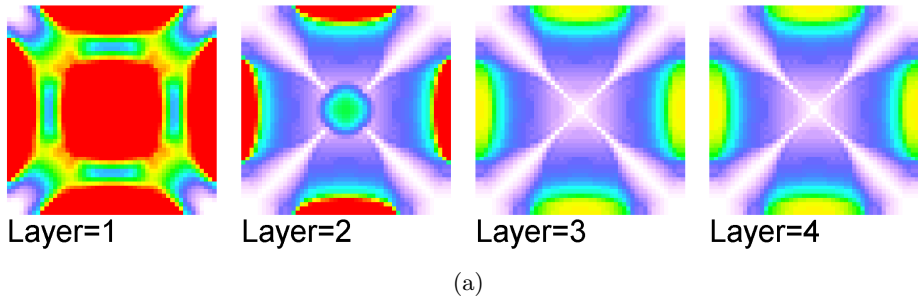
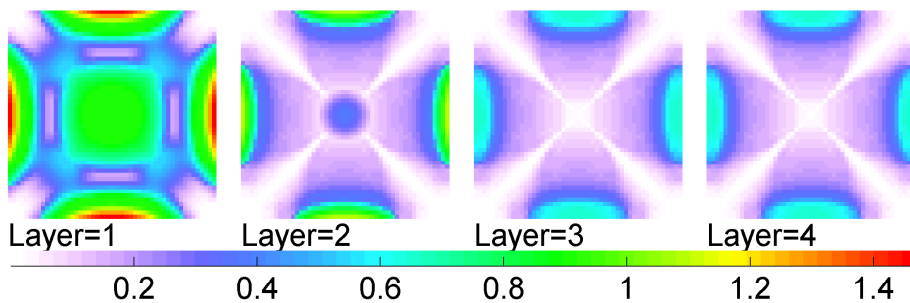
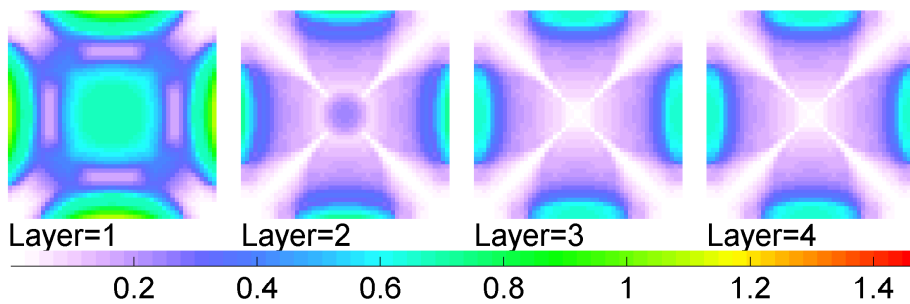


Figure 11: Optimal density distributions of the first four layers for the clamped plate with pressure load, (a) without stress constraints, (b) with stress constraints.

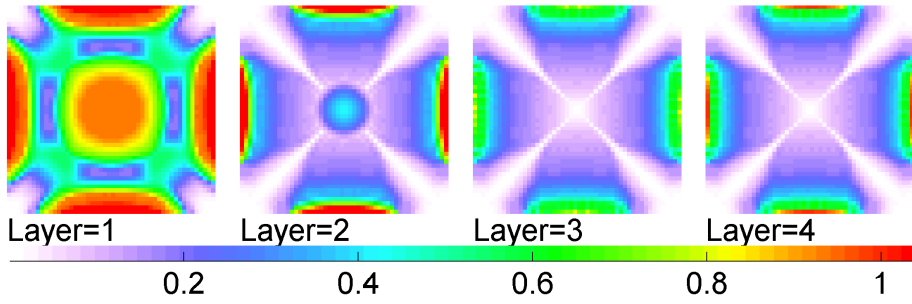


(a)

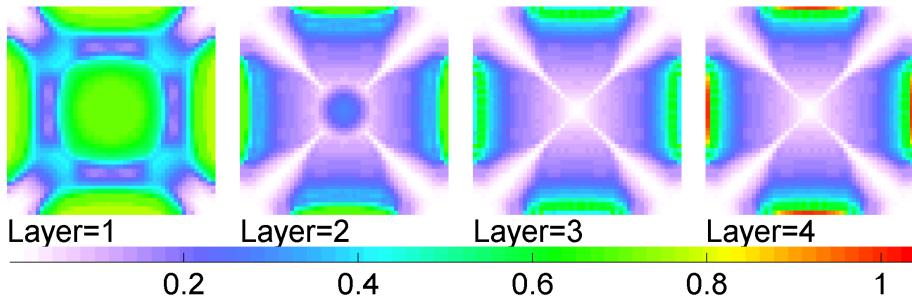


(b)

Figure 12: Optimal stress norms of the first four layers for the clamped plate with pressure load without stress constraints, (a) at the lower surfaces, (b) at the upper surfaces.



(a)



(b)

Figure 13: Optimal stress norms of the <sup>20</sup>first four layers for the clamped plate with pressure load with stress constraints, (a) at the lower surfaces, (b) at the upper surfaces.

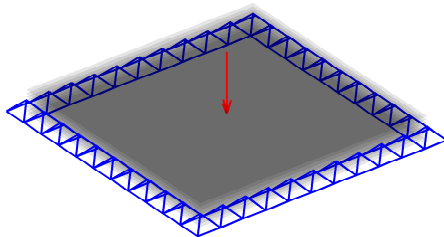


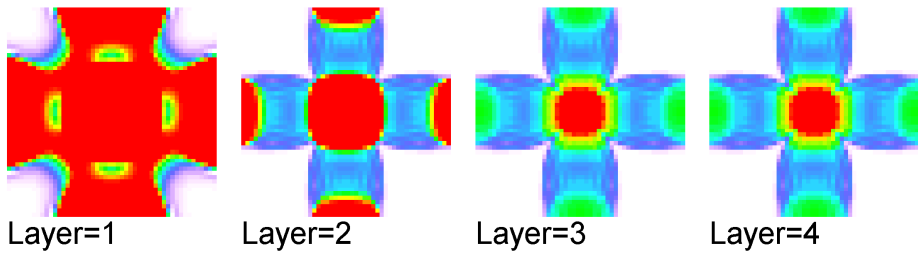
Figure 14: Design domain, boundary condition, and external load for the clamped plate with a point load at the center.

this region are involved in carrying the reduced stress. The density distributions are more or less similar, Figure 15.

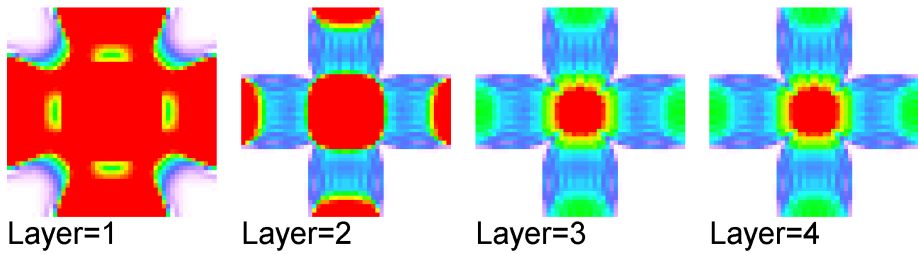
**Example 4.5.** In this example we solve a two load case problem on a shell beam clamped at both ends loaded as in Figure 18. We report the plots for the optimal stress norms of the outer surface for one of the loads. The other cases can easily be determined from these plots. The higher stresses around the loaded region shown in Figure 20a in the unconstrained problem are avoided in the constrained problem, see Figure 20b. There is no clear difference in the topology of the optimal density distributions, Figure 19.

## 5 Conclusions

We introduce stress constraints to the FMO models proposed by the authors in [32] for laminated plates and shells for the first time. We extend the efficient primal-dual interior point method initially developed in [33] for solids and latter generalized in [32] for laminates to solve these stress constrained FMO problems. In the numerical experiments the high stresses in the unconstrained problems which occur mostly near the fixed or loaded areas are reduced in the constrained problems. The feasibility of the stress constraints is higher than we find in other articles (literatures are available only for solids). The number of iterations required to obtain solution to the problems of this article is between 85 and 142. This is modest considering the highly nonlinearity of the stress constraints and non-convexity of the problems. The efficiency of the method is implied indeed.

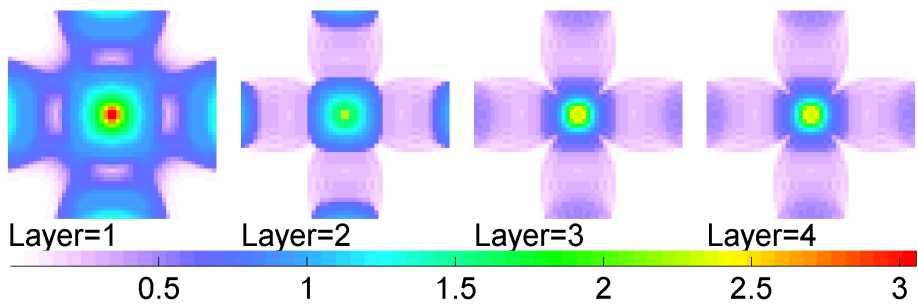


(a)

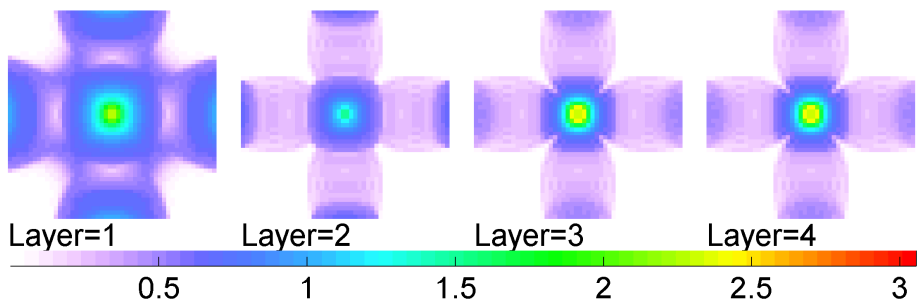


(b)

Figure 15: Optimal density distributions of the first four layers for the clamped plate with load at the center, (a) without stress constraints, (b) with stress constraints.

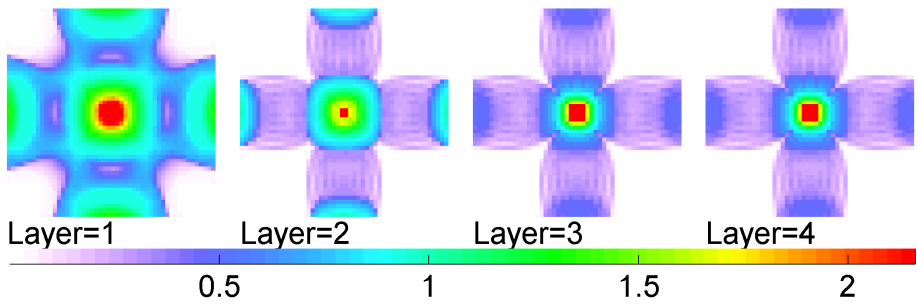


(a)

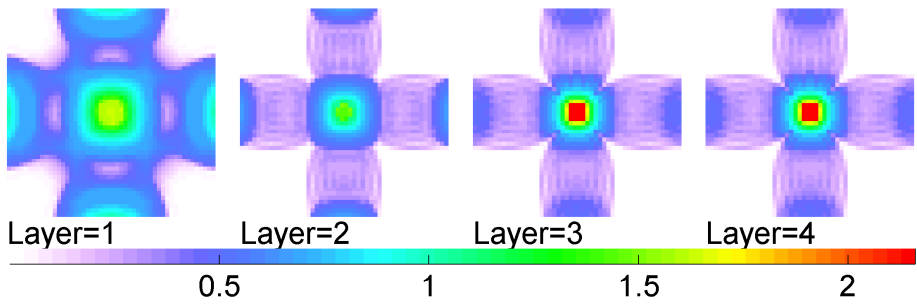


(b)

Figure 16: Optimal stress norms of the <sup>23</sup>first four layers for the clamped plate with load at the center without stress constraints, (a) at the lower surfaces, (b) at the upper surfaces.



(a)



(b)

Figure 17: Optimal stress norms of the first four layers for the clamped plate with load at the center with stress constraints, (a) at the lower surfaces, (b) at the upper surfaces.

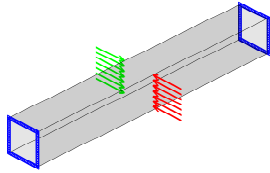
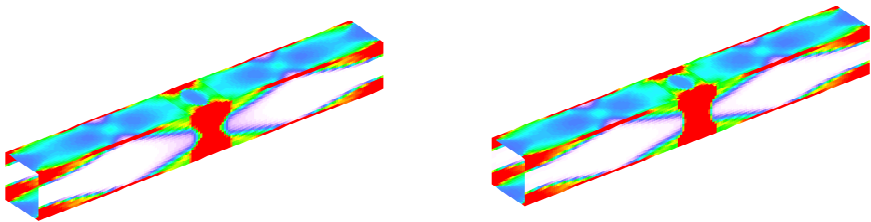


Figure 18: Design domain, boundary condition, and external load for the shell beam.



(a)

(b)

Figure 19: Optimal density distributions for the shell beam, (a) without stress constraints, (b) with stress constraints.

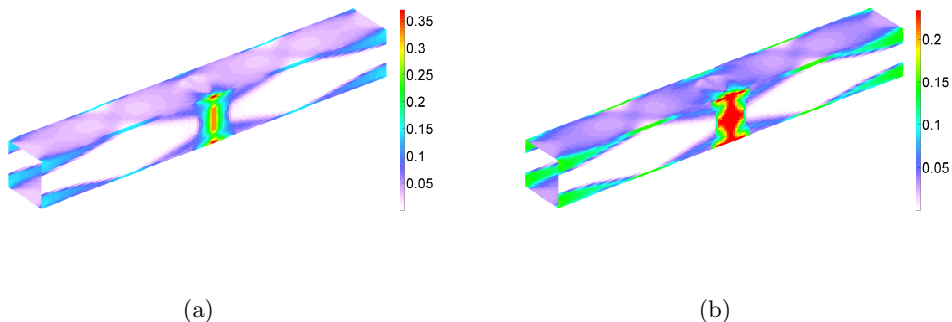


Figure 20: Optimal stress norms for the shell beam, (a) without stress constraints, (b) with stress constraints.

There are two special behaviors that we observed from the numerical experiments. There are (usually) only small differences in the density distributions of the solutions to the constrained and unconstrained FMO problems. This is because in FMO there is more freedom than it is possible to change material properties to avoid the high stresses. This actually contradicts to the practice in classical topology optimization with isotropic materials where the materials are fixed. The second behavior is that we see different practice regarding the compliance in FMO than in other structural optimizations. The values of compliances are only a little relaxed with less than 5% in the constrained problems even when the norm of the stresses are reduced by more than 50%.

We point out two future research areas. The first one is to analyze solutions to FMO problems on laminates. This will give a direction to identify the way stresses are reduced in FMO approach to laminates. The second future research work is on improving the computational efficiency of the algorithm. Stress constraints are in most cases active only in a certain regions in the design domain. Therefore, treating these constraints over the entire design domain in the algorithm is not numerically efficient. The algorithm can be improved by introducing active set technique where inactive stress constraints are removed during the optimization process.

## Acknowledgments

I would like to express my sincere gratitude to Mathias Stolpe for his constructive comments and discussions throughout the entire process of producing the article.

My special thanks also go to my colleagues José Pedro Blasques and Robert Bitsche for many and fruitful discussions on laminated composite structures.

## References

- [1] Achtziger, W., Kanzow, C.: Mathematical programs with vanishing constraints. *Mathematical Programming* **114**(1), 69–99 (2008)
- [2] Bendsøe, M.P., Díaz, A.R.: Optimization of material properties for Mindlin plate design. *Structural Optimization* **6**, 268–270 (1993)
- [3] Bendsøe, M.P., Guedes, J.M., Haber, R.B., Pedersen, P., Taylor, J.E.: An analytical model to predict optimal material properties in the context of optimal structural design. *Journal of Applied Mechanics* **61**, 930–937 (1994)
- [4] Chapelle, D., Bathe, K.J.: *The Finite Element Analysis of Shells - Fundamentals*. Springer, Heidelberg (2003)
- [5] Cheng, G.D., Guo, X.:  $\varepsilon$ -relaxed approach in structural topology optimization. *Structural Optimization* **13**, 258–266 (1997)
- [6] Cook, R.D., Malkus, D.S., Plesha, M.E., Witt, R.J.: *Concepts and Applications of Finite Element Analysis*, 4th edn. John Wiley and Sons (2002)
- [7] Duysinx, P., Bendsøe, M.P.: Topology optimization of continuum structures with local stress constraints. *International Journal for Numerical Methods in Engineering* **43**, 1453–1478 (1998)
- [8] Forsgren, A.: Inertia-controlling factorizations for optimization algorithms. *Applied Numerical Mathematics* **43**, 91–107 (2002)
- [9] Gaile, S.: *Free material optimization for shells and plates*. Ph.D. thesis, Institute of Applied Mathematics II, Friedrich-Alexander University of Erlangen-Nuremberg (2011)
- [10] Guo, X., Cheng, G., Yamazaki, K.: A new approach for the solution of singular optima in truss topology optimization with stress and local buckling constraints. *Structural and Multidisciplinary Optimization* **22**, 364–372 (2001)
- [11] Haslinger, J., Kočvara, M., Leugering, G., Stingl, M.: Multidisciplinary free material optimization. *SIAM Journal on Applied Mathematics* **70**(7), 2709–2728 (2010)

- [12] Hinton, M.J., Kaddour, A.S., Soden, P.D.: Failure criteria in fibre reinforced polymer composites: The world-wide failure exercise. Elsevier, Oxford, UK (2004)
- [13] Kirsch, U.: On singular topologies in optimum structural design. *Structural Optimization* **2**, 133–142 (1990)
- [14] Kočvara, M., Stingl, M.: A code for convex nonlinear and semidefinite programming. *Optimization Methods and Software* **18**(3), 317–333 (2003)
- [15] Kočvara, M., Stingl, M.: Free material optimization for stress constraints. *Structural and Multidisciplinary Optimization* **33**, 323–355 (2007)
- [16] Kočvara, M., Stingl, M.: Mathematical models of FMO with stress constraints FMO. Tech. rep., PLATO-N Public Report PU-R-1-2008 (2009). Available from <http://www.plato-n.org/>
- [17] Kočvara, M., Stingl, M., Zowe, J.: Free material optimization: recent progress. *Optimization* **57**(1), 79–100 (2008)
- [18] Le, C., Norato, J., Bruns, T., Ha, C., Tortorelli, D.: Stress-based topology optimization for continua. *Structural and Multidisciplinary Optimization* **41**, 605–620 (2010)
- [19] Nocedal, J., Wright, S.J.: *Numerical Optimization*. Springer, New York, NY, USA (1999)
- [20] París, J., Navarrina, F., Colominas, I., Casteleiro, M.: Topology optimization of continuum structures with local and global stress constraints. *Structural and Multidisciplinary Optimization* **39**(4), 419–437 (2009)
- [21] Reddy, J.: *Mechanics of laminated composite plates and shells: theory and analysis*, 2nd edn. London (2004)
- [22] Ringertz, U.T.: On finding the optimal distribution of material properties. *Structural Optimization* **5**, 265–267 (1993)
- [23] Rozvany, G.I.N.: Difficulties in truss topology optimization with stress, local buckling and system stability constraints. *Structural Optimization* **11**, 213–217 (1996)
- [24] Stingl, M.: On the solution of nonlinear semidefinite programs by augmented lagrangian method. Ph.D. thesis, Institute of Applied Mathematics II, Friedrich-Alexander University of Erlangen-Nuremberg (2006)

- [25] Stingl, M., Kočvara, M., Leugering, G.: Free material optimization with fundamental eigenfrequency constraints. *SIAM Journal on Optimization* **20**(1), 524–547 (2009)
- [26] Stingl, M., Kočvara, M., Leugering, G.: A new non-linear semidefinite programming algorithm with an application to multidisciplinary free material optimization. *International Series of Numerical Mathematics* **158**, 275–295 (2009)
- [27] Stingl, M., Kočvara, M., Leugering, G.: A sequential convex semidefinite programming algorithm with an application to multiple-load free material optimization. *SIAM Journal on Optimization* **20**(1), 130–155 (2009)
- [28] Stingl, M., Kočvara, M., Leugering, G.: A sequential convex semidefinite programming algorithm with an application to multiple-load free material optimization. *SIAM Journal on Optimization* **20**(1), 130–155 (2009)
- [29] Stolpe, M., Svanberg, K.: On the trajectories of the epsilon-relation relaxation approach for stress-constrained truss topology optimization. *Structural and Multidisciplinary Optimization* **21**, 140–151 (2001)
- [30] Stolpe, M., Svanberg, K.: A note on tress-based truss topology optimization. *Structural and Multidisciplinary Optimization* **25**, 62–64 (2003)
- [31] Wächter, A., Biegler, L.T.: On the implementation of an interior-point filter line-search algorithm for large-scale nonlinear programming. *Mathematical Programming* **106**, 25–57 (2006)
- [32] Weldeyesus, A.G., Stolpe, M.: Free material optimization for laminated plates and shells. Tech. rep., DTU Wind Energy (2014). Submitted
- [33] Weldeyesus, A.G., Stolpe, M.: A primal-dual interior point method for large-scale free material optimization. *Computational Optimization and Applications* (2014). DOI 10.1007/s10589-014-9720-6
- [34] Werner, R.: Free material optimization-mathematical analysis and numerical solution. Ph.D. thesis, Institute of Applied Mathematics II, Friedrich-Alexander University of Erlangen-Nuremberg (2001)
- [35] Yang, B.J., Chen, C.J.: Stress-based topology optimization. *Structural Optimization* **12**, 98–105 (1996)
- [36] Zowe, J., Kočvara, M., Bendsøe, M.P.: Free material optimization via mathematical programming. *Mathematical Programming* **79**, 445–466 (1997)